Desogestrel enhances ventilation in ondine patients: Animal data involving serotoninergic systems

Fanny Joubert, Anne-Sophie Perrin-Terrin, Emilienne Verkaeren, Philippe Cardot, Marie-Noëlle Fiamma, Alain Frugière, Isabelle Rivals, Thomas Similowski, Christian Straus, Laurence Bodineau

Title: Desogestrel enhances ventilation in Ondine patients: animal data involving serotoninergic systems

Authors names and affiliations: Fanny Joubert[1], Anne-Sophie Perrin-Terrin[1,2], Emilienne Verkaeren[1], Philippe Cardot[1], Marie-Noëlle Fiamma[1], Alain Frugière[1], Isabelle Rivals[1,3], Thomas Similowski[1,4,5,#], Christian Straus[1,5,6,#] and Laurence Bodineau[1,*]

[1] Sorbonne Universités, UPMC Univ Paris 06, INSERM, UMR_S1158 Neurophysiologie respiratoire expérimentale et clinique, F-75013, Paris, France; [2] University Paris 13, Sorbonne Paris Cité, Laboratory "Hypoxia & Lung" EA2363, 74 rue Marcel Cachin, 93017, Bobigny, France; [3] Équipe de Statistique Appliquée, ESPCI ParisTech, F-75005 Paris, France, PSL Research University; [4] AP-HP, Groupe Hospitalier Pitié-Salpêtrière Charles Foix, Service de Pneumologie et Réanimation Médicale (*Département "R3S"*), F-75013, Paris, France; [5] AP-HP, Groupe Hospitalier Pitié-Salpêtrière Charles Foix, Branche “Adultes” du Centre de Référence du Syndrome d’Ondine, F-75013, Paris, France; [6] AP-HP, Groupe Hospitalier Pitié-Salpêtrière Charles Foix, Service d’Explorations Fonctionnelles de la Respiration, de l’Exercice et de la Dyspnée (*Département "R3S"*), Paris, France; [#] These authors have contributed equally to this work.

Corresponding author (*): Laurence Bodineau, Sorbonne Universités, UPMC Univ Paris 06, INSERM, UMR_S1158 Neurophysiologie respiratoire expérimentale et clinique, F-75013, Paris, France. Tel 33 1 40 77 97 15, Fax: 33 1 40 77 97 89. E-mail: laurence.bodineau@upmc.fr

Conflict of interest: The authors declare no competing financial interests

Abstract

Central congenital hypoventilation syndrome (CCHS) is a neurorespiratory disease characterized by life-threatening sleep-related hypoventilation involving an alteration of CO_2/H^+ chemosensitivity. Incidental findings have suggested that desogestrel may allow recovery of the ventilatory response to CO_2. The effects of desogestrel on resting ventilation have not been reported. This study was designed to test the hypothesis that desogestrel strengthens baseline ventilation by analyzing the ventilation of CCHS patients. Rodent models were used in order to determine the mechanisms involved. Ventilation in CCHS patients was measured with a pneumotachometer. In mice, ventilatory neural activity was recorded from *ex vivo* medullary-spinal cord preparations, ventilation was measured by plethysmography and *c-fos* expression was studied in medullary respiratory nuclei. Desogestrel increased baseline respiratory frequency of CCHS patients leading to a decrease in their $P_{ET_{CO_2}}$. In medullary spinal-cord preparations or *in vivo* mice, the metabolite of desogestrel, etonogestrel, induced an increase in respiratory frequency that necessitated the functioning of serotoninergic systems, and modulated $GABA_A$ and NMDA ventilatory regulations. c-FOS analysis showed the involvement of medullary respiratory groups of cell including serotoninergic neurons of the *raphe pallidus* and *raphe obscurus* nuclei that seem to play a key role. Thus, desogestrel may improve resting ventilation in CCHS patients by a stimulant effect on baseline respiratory frequency. Our data open up clinical perspectives based on the combination of this progestin with serotoninergic drugs to enhance ventilation in CCHS patients.

Keywords: central congenital hypoventilation syndrome; etonogestrel; *ex vivo* medullary-spinal cord preparations; *in vivo*; progestin; mice.

Highlights

-Desogestrel enhances basal ventilation in Ondine's curse

-Etonogestrel increased respiratory frequency by medullary mechanisms

-$GABA_A$ and NMDA receptors are involved in the respiratory effect of etonogestrel

-5-HT systems are implicated on the effect of etonogestrel on basal ventilation

-Combining 5-HT and desogestrel may constitute a therapeutic utility in Ondine's curse

Abbreviations: aCSF, artificial cerebrospinal fluid; CCHS, congenital central hypoventilation syndrome; CVD, central ventilatory drive; DMSO, dimethylsulfoxide; DSG, desogestrel; ETO, etonogestrel; f_R, respiratory frequency; IntC4, integrated C4 burst activity; NMDA, N-methyl-D-aspartate; NTS, nucleus tractus solitaries; $P_{ET}CO_2$; end-tidal carbon dioxide partial pressure; PBS, phosphate-buffered saline; preBotC, pre-Botzinger complex; RMg, raphe magnus; ROb, raphe obscurus; RPa, raphe pallidus; RTN/pFRG, retrotrapezoid nucleus/parafacial respiratory group; $\dot{V}_E$, minute ventilation; VLM, ventrolateral medullary reticular nucleus; V_T, volume tidal; 5-HT, serotonin.

1. Introduction

Breathing depends on a rhythmic command originating in a brainstem neuronal network that is finely tuned to variations of O_2, CO_2 and pH (Feldman et al., 2013). Significant disruptions in the neuronal respiratory network or its regulatory processes are associated with various pathological conditions including central hypoventilation syndromes (Carroll et al., 2010;Ramanantsoa and Gallego, 2013). These disorders can be life-threatening and may require mechanical ventilatory assistance. They expose patients to neural damage (Harper et al., 2014) and impair their quality of life. No pharmacological treatment is available for central hypoventilation syndromes.

Congenital central hypoventilation syndrome (CCHS) is a neurorespiratory disease characterized by sleep-related hypoventilation and the absence or reduction in CO_2/H^+ chemosensitivity (Amiel et al., 2003;Weese-Mayer et al., 2010) due to mutations of the *PHOX2B* gene (Amiel et al., 2003). Recovery of CO_2/H^+ chemosensitivity was incidentally observed in two adult CCHS women using desogestrel (DSG) for contraceptive purposes (Straus et al., 2010). In view of the known effects of progesterone on central ventilatory drive (CVD) and despite the absence of known effects of progesterone in CCHS (Behan et al., 2003;Sritippayawan et al., 2002), it was hypothesized that DSG was responsible for restoring the ventilatory response to CO_2 (Straus et al., 2010). Deliberately administering DSG to another patient did not induce any recovery of CO_2/H^+ chemosensitivity (Li et al., 2013). These contradictory findings may be due to the complex nature of the actions of progestins on breathing control, idiosyncrasies or both. The action of DSG (Straus et al., 2010), or rather its metabolite 3-ketodesogestrel (etonogestrel; ETO), a synthetic progestin derived from testosterone

and belonging to the gonane family (Schumacher et al., 2007;Sitruk-Ware, 2008), may involve multiple pathways, as animal studies have revealed that the ventilatory action of progesterone and progestins depends on hypothalamus and brainstem mechanisms (Bayliss et al., 1990;Pascual et al., 2002) related to both genomic (Schumacher et al., 2007) and non-genomic effects (Belelli and Lambert, 2005;Pang et al., 2013;Pascual et al., 2002;Ren and Greer, 2006). A better understanding of the mechanisms of action of DSG and ETO on breathing command and regulation is fundamental to evaluate the conditions under which these progestins could be used to treat patients with central hypoventilation. In this context, we recently showed, in rodents, that ETO enhances the ventilatory response to metabolic acidosis by a mechanism involving supramedullary structures (Loiseau et al., 2014). Whether or not DSG and ETO interfere with generation of the respiratory rhythm (namely resting ventilation) is currently unknown.

The present study examined the effect of DSG on resting ventilation in CCHS women and the actions of its metabolite, ETO, on CVD at the medulla oblongata, the anatomical region where essential respiratory neural structures are located (Feldman et al., 2013). The *ex vivo* mouse medullary-spinal cord preparation was used to identify the medullary effects of ETO (Voituron et al., 2011). Combined co-applications of ETO and $GABA_A$ergic, glutamatergic and serotoninergic agonists or antagonists and c-FOS analysis were used to identify the mechanisms involved. Some of the results of these studies have been previously reported in the form of abstracts (Joubert et al., 2014;Perrin-Terrin et al., 2015).

2. Materials and Methods

2.1. Humans

The study in humans was carried out on the ventilatory signal recorded by Straus et al. (Straus et al., 2010) at the time of the first description of recovery of chemosensitivity in two CCHS patients taking DSG 75µg daily for contraception. The previous publication (Straus et al., 2010) reported the ventilatory response of patients to hypercapnia. In the present study, we analyzed the baseline ventilation recorded before exposure to hypercapnia.

The two patients were regularly assessed in the adult branch of the French reference Center for CCHS (Straus et al., 2010;Trang et al., 2005), according to current guidelines (Weese-Mayer et al., 2010). Both patients gave their written consent to scientific publication of the results obtained from their data (Straus et al., 2010).

Briefly, the first patient was a 19-year-old woman, who harbored a 5-alanine expansion mutation of the *PHOX2B* gene. At the time of the study, she was dependent on mechanical ventilation only during sleep and presented normal ventilation during wakefulness at rest.

The second patient was a 30-year-old woman, who harbored a 6-alanine expansion mutation of the *PHOX2B* gene. At the time of the study, she was still tracheotomized and dependent on mechanical ventilation, but only during sleep. However, hypoventilation was present during wakefulness at rest ($P_aO_2 \approx 75$ mmHg; $P_aCO_2 \approx 55$ mmHg).

The two patients breathed through a pneumotachometer and their tidal volume (V_T), respiratory frequency (f_R), minute ventilation ($\dot{V}_E$), and end-tidal carbon dioxide partial pressure ($P_{ET_{CO_2}}$) were recorded (Hyp'Air Compact+, Medisoft, Sorinnes-Dinant,

Belgium) at different times during 5 respiratory cycles, *i.e.* before, during and after DSG exposure.

2.2. Animals

Experiments were performed on both male and female newborn (0-3 days old; 2.1±0.1g) wild-type mice (*Mus musculus*, OF1 strain; Charles River laboratories, L'Arbresle, France (http://www.criver.com/products-services/basic-research/find-a-model/of1-mouse)). All experiments were carried out in accordance with Directive 2010/63/EU of the European Parliament and of the Council of 22 September 2010 and French law (2013/118). All efforts were made to minimize the number of animals used and their suffering. Animals were kept on a 12-hour light-dark cycle with free access to food and water.

2.2.1. Pharmacological agents

Drugs obtained from Sigma-Aldrich (Saint-Quentin Fallavier, France), were prepared in either saline or dimethylsulfoxide (DMSO) and were dissolved in artificial cerebrospinal fluid (aCSF) for *ex vivo* preparations and in oil for *in vivo* experimentations (Garcia-Pelaez et al., 2007;Ren and Greer, 2006). Bicuculline, MK-801, methysergide, N-methyl-D-aspartate (NMDA), muscimol and serotonin (5-hydroxytryptamine, 5-HT) were prepared in saline. ETO, like other steroids, was dissolved in DMSO or oil.

2.2.2. Whole body plethysmography

Animals were placed in an experimental chamber (20mL) in which they could freely move. The chamber was maintained at 33℃, the therm oneutral zone (Gordon and ., 1993), with an external heat source. During the experimental period, the chamber was continuously flushed at $0.6 L \cdot min^{-1}$ for the continuous delivery of air and removal of expired CO_2. Using an adaptation of the barometric method previously described

(Bartlett, Jr. and Tenney, 1970), the pressure change induced by the respiratory flow was recorded with a differential pressure transducer (Valydine MP 45, Northridge, CA, USA). The pressure signal was digitized through a LabChart data analysis system (ADInstruments, Castle Hill, Australia). Measurements were made on 15 sec, at intervals of 5 min.

2.2.3. Medullary-Spinal Cord Preparations

Newborn mice were placed under deep cold anesthesia and medullary-spinal cord preparations were dissected out as previously described. The rostral section was made at the level of the eighth cranial nerve exit point. The caudal section was made between the seventh and eighth cervical spinal roots. Preparations were placed in a recording chamber with the ventral surface facing upward. They were continuously superfused at a rate of 10 ml/min, at 26°C, with di oxygenated aCSF (129.0 mM NaCl, 3.35 mM KCl, 1.26 mM $CaCl_2$ $2H_2O$, 1.15 mM $MgCl_2$ $6H_2O$, 0.58 mM $NaH_2PO_4H_2O$, 21.0 mM $NaHCO_3$, 30.0 mM d-glucose) saturated with O_2 and adjusted to pH 7.4 by bubbling with 95% O_2 and 5% CO_2 (normal pH-aCSF).

CVD was analyzed by measuring the electrical activity of a fourth cervical ventral nerve root (C4) recorded using a suction electrode, filtered (10-3000 Hz), amplified (x5000), integrated (time constant 100 ms) and digitized by a Spike 2 data analysis system (CED, Cambridge, UK), at a sampling frequency of 2500 Hz. As previously reported, f_R was commonly defined as the burst frequency recorded from C4 over 1 minute. The integrated C4 burst activity (IntC4) was also used as an index of inspiratory activity (Voituron et al., 2006).

2.2.4. Pharmacological applications

2.2.4.1. Analysis of the effect of ETO on in vivo newborn mice

Newborn mice received *per os* either ETO (10^{-3}mg/kg) dissolved in oil, or oil alone.

2.2.4.2. Analysis of the effect of ETO on ex vivo preparations

After completion of the surgical procedure, *ex vivo* preparations were maintained in normal pH-aCSF superfusion for 30 minutes to stabilize CVD; baseline values were defined as the mean value over the last 5 minutes of this period. The effect of ETO was determined under normal pH at 0.05, 0.5, 1 and 2µM (final concentration of DMSO used to dissolve ETO was 0.01%). After stabilization, ETO or DMSO alone was added to normal pH-aCSF for 30 minutes. f_R and IntC4 were then averaged over successive 5-minutes intervals and expressed as a percentage of baseline values. Preparations were then either returned to normal pH-aCSF superfusion for 30 minutes or fixed by incubation in 4% paraformaldehyde in 0.1 M phosphate-buffered saline (PBS; pH 7.4).

Analysis of interactions of ETO with $GABA_A$ receptors on ex vivo preparations

In a first step, we investigated possible interactions between $GABA_A$ receptors and ETO by evaluating changes in the effect of ETO under conditions of $GABA_A$ receptor blockade. After stabilization, preparations were successively superfused with normal pH-aCSF containing bicuculline for 10 minutes followed by normal pH-aCSF containing bicuculline and supplemented with ETO or DMSO for 30 minutes; f_R, the only respiratory variable affected by ETO, was expressed as a percentage of bicuculline values (values obtained during the last 5 minutes of bicuculline exposure). Preparations were subsequently returned to normal pH-aCSF for 10 minutes.

In a second set of experiments, we tried to characterize the action of ETO on the $GABA_A$ receptor effects on f_R *i.e.* facilitation or moderation. We compared the effect of muscimol on f_R in both the presence and the absence of ETO. According to data of the literature, the IC_{50} of muscimol was first determined by examining its effect on f_R at several concentrations (0.05, 0.10, 0.15, 0.20 and 0.25µM) for 4 minutes.

Preparations were exposed to normal pH-aCSF containing either ETO or DMSO and then to normal pH-aCSF containing ETO or DMSO with muscimol at IC_{50} for 4 minutes; f_R was expressed as a percentage of pre-muscimol values (values obtained during the 5 minutes preceding muscimol exposure). Preparations were subsequently returned to normal pH-aCSF for 10 minutes.

2.2.4.3. Analysis of interactions of ETO with NMDA receptors on ex vivo preparations

According to data of the literature, the EC_{50} of the effect of NMDA on f_R was determined by examining its effect at several concentrations (8.0, 8.5, 9.0, 9.5 and 10µM) for 10 minutes.

First, we evaluated changes in the effect of ETO under conditions of NMDA receptor blockade. We determined the lowest concentration of MK-801 that totally antagonized the NMDA effect on f_R. Preparations were successively exposed to several concentrations of MK-801 (2.5, 5 and 10µM) for 10 minutes followed by NMDA at EC_{50} for 10 minutes; the lowest concentration of MK-801 that totally antagonized NMDA receptors was found to be 2.5µM. Then, after a stabilization period, preparations were superfused with normal pH-aCSF containing MK-801 (2.5µM) for 10 minutes followed by normal pH-aCSF containing MK-801 supplemented with ETO for 30 minutes; f_R was expressed as a percentage of MK-801 values. Preparations were subsequently returned to normal pH-aCSF for 10 minutes.

Second, to investigate possible modulation of the effects of NMDA receptors on f_R by ETO, we compared the effect of NMDA in both the presence and the absence of ETO. Preparations were exposed to NMDA at EC_{50} for 10 minutes after 30 minutes of exposure to normal pH-aCSF containing either ETO or DMSO; f_R was expressed as a percentage of pre-NMDA values (values obtained during the 5 minutes

preceding NMDA exposure). Preparations were subsequently returned to normal pH-aCSF for 10 minutes.

2.2.4.4. Analysis of interactions of ETO with serotoninergic systems on ex vivo preparations

To study the implication of serotoninergic systems on modulation of central respiratory drive by ETO, we evaluated the effect of ETO in the presence of blockade of 5-$HT_{1/2/7}$ receptors, which are the main 5-HT receptors involved in respiratory modulation (Hilaire and Duron, 1999).

We determined the effect of 5-HT (25µM) for 10 minutes on f_R. We then determined the lowest concentration of methysergide that totally antagonized the respiratory effects of 5-HT. Preparations were successively exposed to several concentrations (1, 2.5, 5 and 10µM) of methysergide for 10 minutes followed by 5-HT (25µM) for 10 minutes; the lowest concentration of methysergide that totally antagonized the effects of 5-HT on f_R was determined to be 5µM.

After a stabilization period, preparations were successively superfused with normal pH-aCSF containing methysergide (5µM) followed by a normal pH-aCSF containing methysergide supplemented with ETO for 30 minutes; f_R was expressed as a percentage of baseline values minus the effect of methysergide alone.

2.2.5. Immunohistochemistry

To identify ETO-induced changes in cell activity, immunohistochemical analysis for c-FOS was carried out in *ex vivo* medullary-spinal cord preparations exposed to either ETO or DMSO for 30 minutes (n=32). At the end, preparations were fixed in 4% paraformaldehyde in 0.1 M PBS (pH 7.4) for 48 hours at 4℃. Preparations were then cryoprotected for 48 hours in 30% sucrose in 0.1 M PBS and stored at -20℃ for subsequent use. Standard immunohistochemical procedures were used to locate c-

FOS on 40µm-thick coronal free-floating sections obtained using a cryostat (Leica CM 1510S) (Voituron et al., 2011). Briefly, sections were incubated with a rabbit polyclonal antibody against c-FOS (sc-52; Santa Cruz Biotechnology Inc., Santa Cruz, CA, USA; 1:2000) in 1% BSA for 48 hours at 4°C. They were then incubated for 2 hours with a biotinylated goat anti-rabbit immunoglobulin (Vector Laboratories, Burlington, Canada; 1:500) and then with an avidin-biotin-peroxidase complex (ABC; Novostain Super ABC kit, Novocastra Laboratories, Newcastle, UK; 1:250) for 1 hour. Peroxidase activity was detected with 0.02% 3,3'-diaminobenzidine tetrahydrochloride and 0.01% H_2O_2 in 0.05M Tris-HCl buffer (pH 7.6).

To characterize the cells displaying changes in activity revealed by c-FOS analysis, dual detections were performed *i.e.* c-FOS and tyrosine hydroxylase (TH) and c-FOS and 5-HT. Sections were first incubated with a rabbit polyclonal antibody against c-FOS (sc-253 Santa Cruz Biotechnology Inc., Santa Cruz, CA, USA; 1:8000; 48 hours; 4℃), then with a biotinylated goat anti-rab bit immunoglobulin (Vector Laboratories, Burlington, Canada; 1:500; 2 hours) and ABC (1:250). Peroxidase activity was detected with 0.02% 3,3'-diaminobenzidine tetrahydrochloride, 0.04% nickel ammonium sulfate and 0.01% hydrogen peroxide in 0.05M Tris buffer (pH 7.6). Secondly, sections were incubated with either a mouse polyclonal antibody against TH (MAB318, Millipore, 1:4000) or a rabbit polyclonal antibody against 5-HT (S5545, Sigma–Aldrich, Saint-Quentin Fallavier, France; 1:500) for 48 hours at 4℃. Sections were subsequently incubated for 2 hours with biotinylated horse anti-mouse (Vector Laboratories, Burlington, Canada; 1:500) or goat anti-rabbit (Vector Laboratories, Burlington, Canada; 1:500), respectively, and then with ABC (1:250). Peroxidase activity was detected with 0.02% 3,3'-diaminobenzidine tetrahydrochloride and 0.01% hydrogen peroxide in 0.05M Tris buffer (pH 7.6).

In all cases, control sections were processed in parallel, but with the omission of primary or secondary antibodies. No labeling was observed on control sections.

Sections were mounted in sequential caudo-rostral order on silanized slides, air-dried and coverslipped with Entellan® (VWR International S.A.S).

Sections were examined under a light microscope (Leica DM 2000, Leica Microsystems, Heidelberg, Germany). The distribution of c-FOS, c-FOS/TH and c-FOS/5-HT immunolabeled cells was plotted onto drawings with the aid of a drawing tube attached to the microscope (magnification x10). c-FOS and double-labeled cells were visually counted under the microscope at high magnification (x400) in medullary structures involved in central respiratory drive using standard landmarks (Paxinos et al., 2007;Paxinos and Franklin, 2001). Immunolabeled cells were photographed with a digital camera (Leica DFC450C, Leica Microsystems, Heidelberg, Germany). c-FOS-positive cells were analyzed in the ventrolateral medullary reticular nucleus (VLM), nucleus tractus solitarius (NTS), medullary raphe nuclei (raphe magnus (RMg), obscurus (ROb) and pallidus (RPa)), retrotrapezoid nucleus/parafacial respiratory group (RTN/pFRG), parapyramidal area (PP), hypoglossal and facial nucleus. The VLM is a neuronal column ventral to the nucleus ambiguus including the pre-Botzinger complex (preBotC) and A1C1 group of neurons and extending from the pyramidal decussation to the caudal edge of the facial nucleus. Using standard landmarks (Paxinos et al., 2007;Paxinos and Franklin, 2001), a distinction was made between the caudal part of the RPa and ROb (from the pyramidal decussation to the rostral edge of the inferior olives) and their rostral part (from the rostral edge of the inferior olives to the rostral edge of the facial nucleus). Several subdivisions of the NTS were analyzed, *i.e* the commissural, median and ventrolateral and the

commissural and median subdivisions were grouped in a single entity referred to as the commissural/median NTS (c/mNTS).

2.2.6. Statistics

Data were expressed as mean (±SEM) and analyzed with GraphPad (GraphPad Prism5 San Diego California USA) or Matlab (MATLAB Version: 8.5.0.197613 (R2015a)).

For human data, the significance of the effects on the responses (f_R, V_T, $\dot{V}_E$ $P_{ET}CO_2$) of the fixed effect time factor (before, during or after DSG treatment) and of the random effect patient factor (two modalities, first or second patient) were tested using a hierarchical two-way ANOVA, homoscedasticity being assessed by Bartlett's test, and normality by Lilliefors' variant of Kolmogorov-Smirnov's test. The p-values of the two-by-two comparisons between different times for each patient were adjusted for multiple testing using Sidak's correction. For animal data, a single dose of each tested drug was applied for each animal or preparation. Depending on normality and homoscedasticity, two-way ANOVA followed by Bonferroni's *post hoc* least squares differences (PLSD) correction or Kruskal-Wallis test followed by Dunn's PLSD were used. Differences were considered significant at $p < 0.05$.

3. Results

3.1. Effect of DSG on baseline ventilatory variables of two CCHS patients

Before DSG exposure, the first CCHS patient displayed a $\dot{V}_E$ of 8.33±0.36L/min resulting from a f_R of 13.06±0.54/min and a V_T of 0.64±0.03L. Her $P_{ET_{CO_2}}$ was 37.33±0.23mmHg. Eighteen months after starting DSG (Straus et al., 2010), baseline f_R increased (17.26±0.66/min, +32%; $p<0.01$; Fig. 1A), $P_{ET_{CO_2}}$ decreased (34.63±0.37mmHg, -7%; $p<0.01$; Fig. 1C), but V_T remained unchanged (0.66±0.02 L), resulting in an increase in $\dot{V}_E$ (11.42±0.25L/min, +37%; $p<0.001$). Four months after stopping DSG, f_R and $\dot{V}_E$ returned to baseline levels (13.34±0.90/min, 8.98±0.29L/min; $p<0.01$; Fig. 1A) and $P_{ET_{CO_2}}$ increased to 42.53±0.45mmHg ($p<0.001$; Fig. 1C).

The second patient presented a similar response profile. Her baseline ventilatory variables were 18.02±0.57/min, 0.60±0.03L and 10.69±0.49L/min for f_R, V_T and $\dot{V}_E$, respectively. Her $P_{ET_{CO_2}}$ was 52.90±0.30mmHg. Two months after starting DSG, f_R increased (27.36±1.71/min, +52%; $p<0.001$; Fig. 1B), but V_T remained unchanged (0.61±0.04L), resulting in an increase in $\dot{V}_E$ (16.53±0.64L/min, +55%; $p<0.001$), while $P_{ET_{CO_2}}$ decreased (46.86±0.45mmHg, -11%; $p<0.001$; Fig. 1D). Two months after stopping DSG, f_R significantly decreased (24.00±0.97/min; $p<0.05$; Fig. 1B) and $\dot{V}_E$ was slightly lower than on DSG (16.45±0.61L/min) but still increased. $P_{ET_{CO_2}}$ increased to 54.36±0.79mmHg ($p<0.001$; Fig. 1D).

3.2. Effect of ETO on baseline respiratory frequency on *in vivo* newborn mice

After exposure to 10^{-3}mg/kg ETO, the baseline f_R was 196.6±12.1cycle/min (Fig. 2B,C; n=11). This f_R was significantly increased compared to control mice (oil exposure; 146.8±7.2cycle/min, $p<0.001$; Fig. 2A,C; n=16).

3.3. Effect of ETO on *ex vivo* preparations

Baseline f_R was 8.5±0.2 bursts/min with no significant differences between groups.

3.3.1. Effect of ETO on CVD

f_R was significantly increased after 25 minutes of exposure to 0.05, 0.5, 1 and 2µM ETO (129.7±5.7%, p<0.001, n=16; 129.7±8.6%, p<0.001, n=14; 123.2±3.2%, p<0.001, n=24 and 147.1±5.8%, p<0.001, n=14, respectively; Fig. 3C-K), while in control, DMSO exposure, did not induce any significant changes (111.0±3.7%, n=18; Fig. 3A,B,K). f_R was significantly higher at all ETO concentrations than with DMSO (0.5 and 1µM p<0.01; 0.05 and 2µM, p<0.001; Fig. 3K). In addition, the increase in f_R induced by 2µM ETO was significantly greater than that observed with lower concentrations (p<0.01, Fig. 3K). After removing the ETO by returning to normal-pH-aCSF, f_R returned to baseline values for 0.05 and 0.5µM ETO, but not for 1 and 2µM ETO (153.1±1.2% and 154.3±14.3%, p<0.05, respectively).

In contrast, the burst amplitude (IntC4) was not modified by ETO (100.9±4.9%; 100.4±1.5%; 98.1±2.7%; 94.2±3.3% for 0.05, 0.5, 1 and 2µM ETO and 99.7±2.2%, for DMSO; Fig. A-J).

3.3.2. Interaction of ETO with the $GABA_A$ receptor

After 10 minutes of exposure, bicuculline ($GABA_A$ receptor antagonist) induced a significant increase in f_R (137.7±8.0%, p<0.001; Fig. 4A,C,E).

Under bicuculline, 0.05µM ETO still induced a significant increase in f_R (115.7±2.8%, p<0.05, n=8; Fig. 4C,D,G) that was significantly different from that observed with DMSO (107.6±3.3%, p<0.05, n=10; Fig. 4A,B), but significantly lower (50%) than the f_R increase induced by ETO without bicuculline (p<0.05; Fig. 4G). After removing the ETO, f_R returned to bicuculline values (97.0±1.8%). In contrast,

under bicuculline, 2µM ETO failed to induce any increase in f_R (107.6±1.1%, p<0.001, n=9; Fig. 4E,F,G).

f_R was dose-dependently decreased by application of muscimol ($GABA_A$ receptor agonist; IC_{50}=0.14µM, n=28; Fig. 4H). The decrease in f_R induced by muscimol (IC_{50}) was greater with ETO (39.6±7.1%, p<0.001, n=14 and 36.7±7.0%, p<0.001, n=14 for 0.05 and 2µM, respectively, Fig. 4K-O) than with DMSO (66.6±11.0%, p<0.01, n=9; Fig. 4I,J,O). After return to normal-pH-aCSF, f_R returned to pre-muscimol values (102.8±2.6% for DMSO and 100.6±3.8% and 112.0±4.0% for 0.05 and 2µM ETO, respectively).

3.3.3. Interaction of ETO with the NMDA receptor

f_R was dose-dependently increased by NMDA (EC_{50}=9.28µM, n=20; Fig. 5A). The optimal concentration of dizocilpine (MK-801, a NMDA receptor antagonist) was 2.5µM. At this concentration, f_R was not significantly altered (103.3±6.1%) and the EC_{50} of NMDA did not modify f_R (113.5±7.8%, n=5). Under 2.5µM MK-801, the increase in f_R induced by 0.05µM ETO was no longer observed (97.6±9.1%, n=4; Fig. 5B-D), this was significantly different from that observed without MK-801 (p<0.01, Fig. 5D).

Exposure to the EC_{50} of NMDA together with DMSO or ETO (0.05 and 2µM) significantly increased f_R (130.4±12.2%, p<0.05, n=10; 153.3±8.8%, p<0.001, n=11; and 140.5±10.2%, p<0.01, n=8, respectively; Fig. 5E-K). The increase in f_R observed with 0.05µM ETO was significantly greater (p<0.05, Fig. 5K) than that observed with DMSO. After return to normal-pH-aCSF, f_R returned to pre-NMDA values for 2µM ETO (91.7±8.8%), but not for DMSO or 0.05µM ETO (80.2±5.3%, p<0.05; 60.8±7.5%, p<0.001; respectively).

3.3.4. Interaction of ETO with serotoninergic systems

5-HT (25µM) increased f_R (146.8±16.4%, p<0.01, n=5; Fig. 6A-C). After exposure to 5µM methysergide (a 5-$HT_{1/2}$ receptor antagonist), mean f_R was not significantly modified by 5-HT (90.7±22.8%, n=3; Fig. 6C).

Under 5µM methysergide, the increase in f_R induced by both 0.05 and 2µM ETO was no longer observed (97.3±2.8%, n=5, and 92.3±3.2%, n=5, respectively, p<0.001; Fig. 6D).

3.3.5. Effect of ETO on the number of c-FOS-positive cells - identification of serotoninergic and catecholaminergic features

0.05µM ETO induced an increase in the number of c-FOS-positive cells in the commissural and median parts of the NTS (c/mNTS; +221±75%, n=12; Table 1; Fig. 7A,E), but not in the ventrolateral part (vlNTS; n=12; Table 1; Fig. 7A,E). Only a very small proportion of cells was also immunoreactive for TH (3.5±2.5%; Fig. 8A-C). 2µM ETO did not induce any change in c-FOS-positive cells in any of the subdivisions of NTS analyzed (n=14; Table 1; Fig. 7A,I).

Both concentrations of ETO induced a significant increase in c-FOS-positive cells in the VLM (+181±55% for 0.05µM and +150±49% for 2µM; Table 1; Fig. 7B,F,J) and a large proportion of these cells was also immunoreactive for TH (42.3±13.5% and 30.7±6.9% at 0.05 and 2µM, respectively; Fig. 8D-F).

ETO induced a significant increase in *c-fos* expression in RPa (Table 1, Fig. 7D,H,L) and ROb (Table 1, Fig. 7C,G,K), but not in RMg (Table 1). This increase was more marked in the caudal part (from the pyramidal decussation to the rostral edge of the inferior olives) than in the rostral part (from the rostral edge of the inferior olives to the rostral edge of the facial nucleus) of the ROb (208±34% *vs* 1176±261% and 344±83% *vs* +834±200% for 0.05 and 2µM ETO, respectively; Table 1, Fig. 7C,G,K),

but not in the RPa (+59±18% *vs* +113±35% and +92±26 *vs* +74±20% for 0.05 and 2µM ETO, respectively; Table 1, Fig. 7D,H,L). A large proportion of c-FOS-positive cells in the caudal parts of RPa and ROb was also immunoreactive for 5-HT (38.4±5.2% and 41.0±9.1% at 0.05µM and 43.6±6.8% and 56.1±6.5% at 2µM, Fig. 9A-F). In contrast, only a few cells in the rostral parts of RPa and ROb were also 5-HT-positive (5.4±0.9% and 23.6±3.8% at 0.05µM and 9.7±3.8% and 15.0±2.2% at 2µM).

ETO exposure also induced a significant increase in *c-fos* expression in facial (+35±8% and +59±14% for 0.05 and 2µM ETO, respectively; Table 1) and hypoglossal (+626±185% and +400±103% for 0.05 and 2µM ETO, respectively; Table 1) nuclei.

On the ventral medullary surface, at the level of the RTN/pFRG and PP (cells located at the lateral edge of the pyramidal tract (Paxinos et al., 2007;Paxinos and Franklin, 2001)), *c-fos* expression was not modified by ETO exposure (Table 1).

4. Discussion

This study was conducted on the basis of clinical observations showing that exposure to a progestin of the gonane family increases f_R in CCHS patients and shows that such molecules can experimentally increase respiratory frequency in newborn mice *in vivo* and in isolated brainstem. Our data demonstrate medullary mechanisms, indicating that serotoninergic neurons within the medullary raphe nuclei are involved.

4.1. DSG accelerates f_R and reduces $P_{ET_{CO_2}}$ in CCHS patients

The first description of the ventilatory effects of DSG in CCHS patients (Straus et al., 2010) focused on chemosensitivity and recovery of a perceptual and ventilatory response to CO_2, mostly because this finding constituted a major surprise. The first patient did not know at all that she was taking a potentially effective drug, but the second patient was aware of the observation made with the first patient and of the hypothesis concerning her own ventilatory response to hypercapnia. Since the observations were not part of a blinded study, but fortuitously observed in a clinical setting, the patients were aware of the drug withdrawal. The effects of DSG on baseline ventilation were not examined in detail. Review of the data collected dynamically (before, during and after DSG exposure) from the same two patients showed that f_R was higher and $P_{ET_{CO_2}}$ was lower in the presence of DSG compared to the absence of DSG (Fig. 1). This evidence is undoubtedly fragile (only two patients, retrospective analysis, absence of control of DSG administration due the serendipitous nature of the observations). The present re-analysis suggests that the ventilatory effect of DSG could extend beyond chemosensitivity, as DSG may increase f_R and lower $P_{ET_{CO_2}}$ during resting breathing in certain CCHS patients despite the defective respiratory rhythmogenesis characteristic of this disease.

Because progesterone and pregnane progestins increase f_R in healthy humans (Behan et al., 2003;Jensen et al., 2008;Skatrud et al., 1978), but not in CCHS patients (Sritippayawan et al., 2002), our observations suggest that DSG and more generally gonane progestins could interfere with breathing control via distinct mechanisms from those involved in the action of pregnanes.

4.2. ETO, the metabolite of DSG, increased the f_R on in vivo newborn mice

In vivo, considering the bioavailability of the DSG, the administration of 10^{-3}mg/kg of ETO is the nearest concentration of the human exposure (Timmer et al., 1999). At this concentration, in newborn mice ETO induced an increase of baseline f_R compared to control (Fig. 2). Although the developmental stage was different, this increase is similar to what we observed in adult CCHS patients (Fig. 1).

4.3. ETO, the metabolite of DSG, enhances f_R via medullary mechanisms

On *ex vivo* preparations containing only the medullary regions of the brainstem, acute exposure to ETO induced a dose-dependent increase in f_R (Fig. 3) with no change in IntC4. This finding resembles our observations in CCHS patients (increased f_R with no V_T changes). The f_R increase in CCHS patients receiving DSG and in *in vivo* newborn mice receiving 10^{-3}mg/kg of ETO (Fig. 1,2) may therefore be mediated by medullary mechanisms.

c-FOS labeling revealed increased cellular activity in the VLM, with 30-40% of c-FOS-positive catecholaminergic cells (Fig. 8), suggesting that catecholaminergic cells are involved in the ETO effects. Numerous data have implicated the A1C1 catecholaminergic cell group in the control of breathing (Erickson and Millhorn, 1994;Johnson et al., 2005;Viemari, 2008). However, at least 60% of VLM c-FOS-positive cells are not catecholaminergic. Of note, the preBotC, one of the two medullary respiratory oscillators (Feldman et al., 2013;Smith et al., 1991), is located

in the VLM and does not contain catecholaminergic cells (Wang et al., 2001). Therefore, part of the non-catecholaminergic c-FOS-positive cells could be neurons of the preBotC. Further experiments are needed to confirm this hypothesis. As we did not observe any change in the number of c-FOS-positive cells in the RTN/pFRG, the second medullary respiratory oscillator (Feldman et al., 2013;Onimaru and Homma, 2003), is unlikely to be involved in the progestin effect. Of note, this structure is missing in transgenic mice harboring the same *Phox2b* mutation as CCHS patients (Dubreuil et al., 2008) and is therefore also probably missing in CCHS patients. Nevertheless, their baseline ventilation increased with DSG, which is consistent with the absence of involvement of the RTN/pFRG in the effects of ETO.

4.4. ETO regulates the efficiency of $GABA_A$- and NMDA-mediated modulation of f_R

Under conditions of bicuculline-induced $GABA_A$ receptor blockade, ETO facilitation was diminished or abolished (Fig. 4). This result suggests that part of the ETO effect on f_R depends on an interaction with $GABA_A$ receptors, which would be consistent with data of literature reporting that steroids, including progesterone and progestins, interact with $GABA_A$ (Belelli and Lambert, 2005;Park-Chung et al., 1999). Steroids are known to be either negative, positive or both allosteric modulators of $GABA_A$ (Park-Chung et al., 1999;Ren and Greer, 2006). No data are available concerning the interaction of ETO with $GABA_A$. Our experiments show that the decrease in f_R induced by the $GABA_A$ agonist muscimol was markedly enhanced by ETO exposure, suggesting that ETO exerts a positive modulation of $GABA_A$. Two elements support this hypothesis. First, testosterone, from which ETO is derived, is a positive modulator of $GABA_A$ (Park-Chung et al., 1999). Second, steroids that are negative modulators of $GABA_A$ are characterized by a negative charge at C-3 (Park-Chung et al., 1999). This is not the case of ETO that displays a keto-group at this site

(Grandi et al., 2014). It is possible that part of the ventilatory effect of ETO depends on positive modulation of $GABA_A$ receptors that contribute to CVD. The differential effects of bicuculline on the ventilatory action of ETO (total or partial blockade) may be due to an ETO concentration-dependent effect on several types of $GABA_A$ receptors, as it has been shown that for some neurosteroids the $GABA_A$-evoked responses mediated by receptors containing $\alpha_{1/3}$ subunits are enhanced by relatively low steroid concentrations. In contrast, equivalent receptors that incorporate $\alpha_{2/4/5/6}$ subunits require higher steroid concentrations (Belelli and Lambert, 2005). According to this hypothesis, differences in the effects of bicuculline on the ventilatory action of ETO may be due to a global efficiency of various types of $GABA_A$ receptors, particularly $\alpha_{1/3}$ $GABA_A$ or $\alpha_{2/4}$ $GABA_A$ that have been either located in medullary respiratory areas or shown to play a role in CVD (Liu and Wong-Riley, 2006;Loria et al., 2013).

Bicuculline-induced $GABA_A$ receptor blockade did not completely abolish the facilitation induced by low ETO concentration (Fig. 4). We therefore hypothesized that other receptors were involved. We focused on NMDA receptors because they are both involved in CVD and are modulated by steroids (Funk et al., 1997;Greer et al., 1991;Korinek et al., 2011). Our experiments showed that NMDA blockade totally abolished the facilitatory influence of ETO on f_R (Fig 5), suggesting that either ETO modulates NMDA regulation of f_R, or that all pathways by which ETO increased f_R require functional glutamate/NMDA neurotransmission, or both. Our results showing that ETO potentiated the NMDA-induced increase in f_R only at low progestin concentrations support the hypothesis of modulation of NMDA regulation of f_R by ETO. c-FOS labeling suggested that ETO modulation of f_R regulation by NMDA depends on the c/mNTS, which was the only area displaying an increase in c-FOS-

positive cells, at low but not at high ETO concentrations. This hypothesis is supported by data indicating that NMDA receptors are present on c/mNTS neurons (Lin et al., 2008) and that the excitatory response of NTS neurons to application of NMDA is modulated by steroids (Xue and Hay, 2003). As the c-FOS-positive neurons of the c/mNTS were not catecholaminergic, ETO is likely to influence another cell population.

4.5. ETO increases f_R via a pathway involving medullary serotoninergic systems

Because blockade of serotoninergic regulation of f_R abolished the facilitatory effect of ETO, we hypothesized that this effect involved serotoninergic signaling, which is in line with published data showing that serotoninergic neurons are involved in the facilitatory influence of progesterone (Behan et al., 2003;Farmer et al., 1996). The effect of steroids on the release of 5-HT depends on supramedullary regions, such as pons (Robichaud and Debonnel, 2004) or hypothalamus (Farmer et al., 1996). Our experiments suggest that ETO interfered with serotoninergic systems via a direct medullary action, revealing a new pathway of interaction between progesteronergic and serotoninergic systems. More specifically, our c-FOS data suggest that ETO exerted its facilitatory action by activating serotoninergic neurons located in the caudal parts of RPa and ROb, two areas known to be implicated in ventilatory control (Cao et al., 2006;Cerpa et al., 2015;Depuy et al., 2011). This progestin-serotonin interaction affecting modulation of CVD would be specific to the gonane family. This putative pathway forms a relevant basis for dedicated investigations designed to elaborate personalized approaches to treat CCHS patients with gonane progestins. Otherwise, serotoninergic and non serotoninergic neurons of the medullary raphe nuclei and particularly those of the rRPa are involved in the processes of thermogenesis and heat conservation (McGlashon et al.,

2015;Nakamura and Morrison, 2007). Thus, *in vivo*, it is quite conceivable that these neurons stimulated by ETO could increase the CVD not only by a direct action on the central respiratory pattern generators but also indirectly by inducing an hyperthermia.

5. Conclusion

To conclude, DSG has been associated with chemosensitivity recovery in CCHS patients (Straus et al., 2010). Its metabolite, ETO, has been shown to enhance chemosensitivity in newborn rats via supramedullary mechanisms (Loiseau et al., 2014). Combined with the present data, these observations suggest that two distinct pathways are involved in the ventilatory effects of these gonane progestins. The medullary pathway described here could be relevant to resting breathing CVD, whereas the supramedullary pathway previously described could be relevant to chemosensitivity. Medullary and supramedullary mechanisms could coexist in CCHS. Their effect on resting breathing are particularly pertinent to the issue of ventilatory support. The present animal data, indicating a medullary serotoninergic determinant of the stimulant effect of ETO, provide a rationale for clinical trials combining DSG and serotoninergic drugs to improve ventilation in CCHS patients.

Acknowledgements: F Joubert was supported by the "Fonds de dotation pour la Recherche en Santé Respiratoire 2012". E Verkaeren was supported by the "Fonds de dotation pour la Recherche en Santé Respiratoire 2014". The present work was supported by a grant from the "Association Française pour le Syndrome d'Ondine", by a "Legs Poix" grant from the "Chancellerie de l'Université de Paris" and by the French government - Institut Hospitalo-Universitaire - A - Institut du cerveau et de la Moelle épinière (IHU-A-ICM) "Investissement d'avenir" ANR-10-IAIHU-06 program. We thank Anthony Saul for the English style.

References

Amiel J, Laudier B, ttie-Bitach T, Trang H, de PL, Gener B, Trochet D, Etchevers H, Ray P, Simonneau M, Vekemans M, Munnich A, Gaultier C, Lyonnet S (2003) Polyalanine expansion and frameshift mutations of the paired-like homeobox gene PHOX2B in congenital central hypoventilation syndrome. Nat Genet 33:459-461.

Bartlett D, Jr., Tenney SM (1970) Control of breathing in experimental anemia. Respir Physiol 10:384-395.

Bayliss DA, Cidlowski JA, Millhorn DE (1990) The stimulation of respiration by progesterone in ovariectomized cat is mediated by an estrogen-dependent hypothalamic mechanism requiring gene expression. Endocrinology 126:519-527.

Behan M, Zabka AG, Thomas CF, Mitchell GS (2003) Sex steroid hormones and the neural control of breathing. Respir Physiol Neurobiol 136:249-263.

Belelli D, Lambert JJ (2005) Neurosteroids: endogenous regulators of the GABA(A) receptor. Nat Rev Neurosci 6:565-575.

Cao Y, Matsuyama K, Fujito Y, Aoki M (2006) Involvement of medullary GABAergic and serotonergic raphe neurons in respiratory control: electrophysiological and immunohistochemical studies in rats. Neurosci Res 56:322-331.

Carroll MS, Patwari PP, Weese-Mayer DE (2010) Carbon dioxide chemoreception and hypoventilation syndromes with autonomic dysregulation. J Appl Physiol (1985) 108:979-988.

Cerpa VJ, Aylwin ML, Beltran-Castillo S, Bravo EU, Llona IR, Richerson GB, Eugenin JL (2015) Prenatal-perinatal Nicotine Alters Neonatal Raphe Neurons: Meaning for Sudden Infant Death Syndrome. Am J Respir Cell Mol Biol.

Depuy SD, Kanbar R, Coates MB, Stornetta RL, Guyenet PG (2011) Control of breathing by raphe obscurus serotonergic neurons in mice. J Neurosci 31:1981-1990.

Dubreuil V, Ramanantsoa N, Trochet D, Vaubourg V, Amiel J, Gallego J, Brunet JF, Goridis C (2008) A human mutation in Phox2b causes lack of CO2 chemosensitivity, fatal central apnea, and specific loss of parafacial neurons. Proc Natl Acad Sci U S A 105:1067-1072.

Erickson JT, Millhorn DE (1994) Hypoxia and electrical stimulation of the carotid sinus nerve induce Fos-like immunoreactivity within catecholaminergic and serotoninergic neurons of the rat brainstem. J Comp Neurol 348:161-182.

Farmer CJ, Isakson TR, Coy DJ, Renner KJ (1996) In vivo evidence for progesterone dependent decreases in serotonin release in the hypothalamus and midbrain central grey: relation to the induction of lordosis. Brain Res 711:84-92.

Feldman JL, Del Negro CA, Gray PA (2013) Understanding the rhythm of breathing: so near, yet so far. Annu Rev Physiol 75:423-452.

Funk GD, Johnson SM, Smith JC, Dong XW, Lai J, Feldman JL (1997) Functional respiratory rhythm generating networks in neonatal mice lacking NMDAR1 gene. J Neurophysiol 78:1414-1420.

Garcia-Pelaez B, Vila R, Remesar X (2007) The administration of oleoyl-estrone to lactating dams induces selective changes in the normal growth pattern of their pups. Horm Metab Res 39:582-588.

Gordon C, . (1993) Metabolism. In: In temperature regulation in laboratory rodents pp 47-72.

Grandi G, Cagnacci A, Volpe A (2014) Pharmacokinetic evaluation of desogestrel as a female contraceptive. Expert Opin Drug Metab Toxicol 10:1-10.

Greer JJ, Smith JC, Feldman JL (1991) Role of excitatory amino acids in the generation and transmission of respiratory drive in neonatal rat. J Physiol 437:727-749.

Harper RM, Kumar R, Macey PM, Woo MA, Ogren JA (2014) Affective brain areas and sleep-disordered breathing. Prog Brain Res 209:275-293.

Hilaire G, Duron B (1999) Maturation of the mammalian respiratory system. Physiol Rev 79:325-360.

Jensen D, Duffin J, Lam YM, Webb KA, Simpson JA, Davies GA, Wolfe LA, O'Donnell DE (2008) Physiological mechanisms of hyperventilation during human pregnancy. Respir Physiol Neurobiol 161:76-86.

Johnson PL, Hollis JH, Moratalla R, Lightman SL, Lowry CA (2005) Acute hypercarbic gas exposure reveals functionally distinct subpopulations of serotonergic neurons in rats. J Psychopharmacol 19:327-341.

Joubert F, Straus C, Similowski T, Bodineau L (2014) Effect of an acute exposure to etonogestrel, a progestin, on the central respiratory drive in mouse, involvement of medullary areas. pp 12.

Korinek M, Kapras V, Vyklicky V, Adamusova E, Borovska J, Vales K, Stuchlik A, Horak M, Chodounska H, Vyklicky L, Jr. (2011) Neurosteroid modulation of N-methyl-D-aspartate receptors: molecular mechanism and behavioral effects. Steroids 76:1409-1418.

Li D, Chin C, Kato R, Ward S, Keens TG (2013) Does desogestrel improve ventilatory control in congenital central hypoventilation syndrome? pp A5194.

Lin LH, Taktakishvili OM, Talman WT (2008) Colocalization of neurokinin-1, N-methyl-D-aspartate, and AMPA receptors on neurons of the rat nucleus tractus solitarii. Neuroscience 154:690-700.

Liu Q, Wong-Riley MT (2006) Developmental changes in the expression of GABAA receptor subunits alpha1, alpha2, and alpha3 in brain stem nuclei of rats. Brain Res 1098:129-138.

Loiseau C, Osinski D, Joubert F, Straus C, Similowski T, Bodineau L (2014) The progestin etonogestrel enhances the respiratory response to metabolic acidosis in newborn rats. Evidence for a mechanism involving supramedullary structures. Neurosci Lett 567:63-67.

Loria CJ, Stevens AM, Crummy E, Casadesus G, Jacono FJ, Dick TE, Siegel RE (2013) Respiratory and behavioral dysfunction following loss of the GABAA receptor alpha4 subunit. Brain Behav 3:104-113.

McGlashon JM, Gorecki MC, Kozlowski AE, Thirnbeck CK, Markan KR, Leslie KL, Kotas ME, Potthoff MJ, Richerson GB, Gillum MP (2015) Central serotonergic neurons activate and recruit thermogenic brown and beige fat and regulate glucose and lipid homeostasis. Cell Metab 21:692-705.

Nakamura K, Morrison SF (2007) Central efferent pathways mediating skin cooling-evoked sympathetic thermogenesis in brown adipose tissue. Am J Physiol Regul Integr Comp Physiol 292:R127-R136.

Onimaru H, Homma I (2003) A novel functional neuron group for respiratory rhythm generation in the ventral medulla. J Neurosci 23:1478-1486.

Pang Y, Dong J, Thomas P (2013) Characterization, neurosteroid binding and brain distribution of human membrane progesterone receptors delta and {epsilon} (mPRdelta and mPR{epsilon}) and mPRdelta involvement in neurosteroid inhibition of apoptosis. Endocrinology 154:283-295.

Park-Chung M, Malayev A, Purdy RH, Gibbs TT, Farb DH (1999) Sulfated and unsulfated steroids modulate gamma-aminobutyric acidA receptor function through distinct sites. Brain Res 830:72-87.

Pascual O, Morin-Surun MP, Barna B, avit-Saubie M, Pequignot JM, Champagnat J (2002) Progesterone reverses the neuronal responses to hypoxia in rat nucleus tractus solitarius in vitro. J Physiol 544:511-520.

Paxinos G, Franklin KB (2001) The mouse brain in stereotaxic coordinates, 2nd Edition. San Diego, CA: Academic Press.

Paxinos G, Halliday G, Watson C, Koutcherov Y, Wang H (2007) Atlas of the developing mouse brain. Academic Press.

Perrin-Terrin AS, Joubert F, Fiamma MN, Cardot P, Frugiere A, Straus C, Bodineau L (2015) Facilitation of the respiratory rhythm in mice by acute exposure to a progestin, the Etonogestrel. Involvement of medullary areas. pp 81-82.

Ramanantsoa N, Gallego J (2013) Congenital central hypoventilation syndrome. Respir Physiol Neurobiol 189:272-279.

Ren J, Greer JJ (2006) Modulation of respiratory rhythmogenesis by chloride-mediated conductances during the perinatal period. J Neurosci 26:3721-3730.

Robichaud M, Debonnel G (2004) Modulation of the firing activity of female dorsal raphe nucleus serotonergic neurons by neuroactive steroids. J Endocrinol 182:11-21.

Schumacher M, Guennoun R, Ghoumari A, Massaad C, Robert F, El-Etr M, Akwa Y, Rajkowski K, Baulieu EE (2007) Novel perspectives for progesterone in hormone replacement therapy, with special reference to the nervous system. Endocr Rev 28:387-439.

Sitruk-Ware R (2008) Pharmacological profile of progestins. Maturitas 61:151-157.

Skatrud JB, Dempsey JA, Kaiser DG (1978) Ventilatory response to medroxyprogesterone acetate in normal subjects: time course and mechanism. J Appl Physiol Respir Environ Exerc Physiol 44:939-944.

Smith JC, Ellenberger HH, Ballanyi K, Richter DW, Feldman JL (1991) Pre-Botzinger complex: a brainstem region that may generate respiratory rhythm in mammals. Science 254:726-729.

Sritippayawan S, Hamutcu R, Kun SS, Ner Z, Ponce M, Keens TG (2002) Mother-daughter transmission of congenital central hypoventilation syndrome. Am J Respir Crit Care Med 166:367-369.

Straus C, Trang H, Becquemin MH, Touraine P, Similowski T (2010) Chemosensitivity recovery in Ondine's curse syndrome under treatment with desogestrel. Respir Physiol Neurobiol 171:171-174.

Timmer CJ, Srivastava N, Dieben TO, Cohen AF (1999) Bioavailability and bioequivalence of etonogestrel from two oral formulations of desogestrel: Cerazette and Liseta. Eur J Drug Metab Pharmacokinet 24:335-343.

Trang H, Dehan M, Beaufils F, Zaccaria I, Amiel J, Gaultier C (2005) The French Congenital Central Hypoventilation Syndrome Registry: general data, phenotype, and genotype. Chest 127:72-79.

Viemari JC (2008) Noradrenergic modulation of the respiratory neural network. Respir Physiol Neurobiol 164:123-130.

Voituron N, Frugiere A, Champagnat J, Bodineau L (2006) Hypoxia-sensing properties of the newborn rat ventral medullary surface in vitro. J Physiol 577:55-68.

Voituron N, Frugiere A, Mc Kay LC, Romero-Granados R, Dominguez-Del-Toro E, Saadani-Makki F, Champagnat J, Bodineau L (2011) The kreisler mutation leads to the loss of intrinsically hypoxia-activated spots in the region of the retrotrapezoid nucleus/parafacial respiratory group. Neuroscience 194:95-111.

Wang H, Stornetta RL, Rosin DL, Guyenet PG (2001) Neurokinin-1 receptor-immunoreactive neurons of the ventral respiratory group in the rat. J Comp Neurol 434:128-146.

Weese-Mayer DE, Berry-Kravis EM, Ceccherini I, Keens TG, Loghmanee DA, Trang H (2010) An official ATS clinical policy statement: Congenital central hypoventilation syndrome: genetic basis, diagnosis, and management. Am J Respir Crit Care Med 181:626-644.

Xue B, Hay M (2003) 17beta-estradiol inhibits excitatory amino acid-induced activity of neurons of the nucleus tractus solitarius. Brain Res 976:41-52.

Figure/Table Legends

Figure 1

DSG increases baseline f_R in two CCHS patients. (A-D) Boxplot showing the median breath-by-breath f_R (A and C) and median breath-by-breath P_{ETCO_2} (B and D) in two CCHS patients. † indicates a significant difference between before or after DSG treatment and during DSG exposure. ANOVA *1 way* – Bonferroni post test. $^{††}p < 0.01$, $^{†††}p < 0.001$; desogestrel (DSG).

Figure 2

ETO increases baseline f_R *in vivo* on newborn mice. (A-B) Traces illustrate baseline f_R of newborn mice after two hours of oil (A) or ETO (B) exposure. (C) Histogram showing mean value of f_R of oil (white bar) or ETO (gray bar) exposure. Date are expressed as mean ± SEM. # indicates a significant difference between oil and ETO values. Student t test; $^{###}p < 0.001$.

Figure 3

ETO increases baseline f_R on *ex vivo* medullary-spinal cord preparations. (A-J) Traces illustrate ventilatory C4 activity under normal-pH-aCSF; traces illustrate the central respiratory drive recorded the last five minutes before (A, C, E, G and I) and during the DMSO (B) or ETO exposure (D, F, H and J). (K) Histogram showing mean value of f_R of DMSO (white bar) or ETO (gray bars) exposure. Data are expressed as mean ± SEM * indicates a significant increase in mean f_R compared to baseline values. # indicates a significant difference between DMSO and ETO values. § indicates a significant difference between ETO 2µM and lower ETO concentrations. ANOVA *2 way* – Bonferroni post test. Integrated activity of C4 ventral nerve root (∫C4); electrical activity of C4 ventral nerve root (C4); ***$p < 0.001$, $^{##}p < 0.01$, $^{###}p < 0.001$, $^{§§}p < 0.01$; etonogestrel (ETO).

Figure 4

ETO regulates the efficiency of $GABA_A$ modulation of f_R. (A-F) Ventilatory C4 activity under bicuculline exposure during the last five minutes preceding (A, C and E); and during (B, D and F) DMSO or ETO exposure. (G) Histogram showing mean value of f_R of ETO exposure without and in presence of bicuculline. (H) Dose response curve of changes in mean f_R in response to exposure to muscimol. (I-N) Traces illustrate the ventilatory C4 activity under DMSO and ETO exposure during the last five minutes preceding (I, K and M) and the last two minutes during (J, L and N) muscimol application. (O) Histogram showing mean value of f_R observed under muscimol and DMSO (white bar) or ETO (gray bars) application. Data are expressed as mean ± SEM. * indicates a significant increase in mean f_R compared to bicuculline or pre-muscimol values. # indicates a significant difference between ETO and ETO-BIC or DMSO exposures. ANOVA *2 way* – Bonferroni post test. Integrated activity of the C4 ventral nerve root (∫C4); electrical activity of the C4 ventral nerve root (C4); $^{**}p < 0.01$, $^{***}p < 0.001$, $^{\#}p < 0.05$, $^{\#\#}p < 0.01$; etonogestrel (ETO); bicuculline (BIC).

Figure 5

ETO regulates the efficiency of NMDA modulation of f_R. (A) Dose response curve of changes in mean f_R in response to exposure to the NMDA receptor agonist NMDA. (B-C) Traces illustrated ventilatory C4 activity under MK-801 exposure during the last five minutes preceding (B) and during (C) ETO exposure. (D) Histogram showing mean value of f_R observed under MK-801 and ETO (gray bars) application. (E-J) Traces illustrated ventilatory C4 activity under DMSO and ETO exposure during the last five minutes preceding (E, G and I) and during (F, H and J) NMDA application. (K) Histogram showing mean value of f_R observed under NMDA and DMSO (white bar) or ETO (gray bars) application. All values are expressed as mean ± SEM. *

indicates a significant increase in mean f_R compared to bicuculline or ETO values. # indicates a significant difference between ETO and DMSO or ETO and ETO-MK 801 exposure. ANOVA *2way* – Bonferroni post test. Integrated activity of C4 ventral nerve root (∫C4); electrical activity of C4 ventral nerve root (C4); **p < 0.01, ***p < 0.001, $^{\#\#}$p < 0.01; etonogestrel (ETO).

Figure 6

Medullary serotoninergic systems are involved in ETO ventilatory effect. (A-B) Traces illustrated ventilatory C4 activity during the last five minutes preceding (A) and during (B) the 5-HT exposure. (C) Histogram showing mean value of f_R observed under 5-HT exposure without and in presence of methysergide (5µM). (D) Histogram showing mean value of f_R over under ETO exposure without and in presence of methysergide. All values are expressed as mean ± SEM. * indicates a significant increase in mean f_R compared to pre-5-HT or baseline values. # indicates a significant difference between presence or absence of methysergide. Kruskal-Wallis – Dunn post test. Integrated activity of C4 ventral nerve root (∫C4); electrical activity of C4 ventral nerve root (C4); **p < 0.01, ***p < 0.001, $^{\#}$p < 0.05, $^{\#\#\#}$p < 0.001; etonogestrel (ETO); serotonin (5-HT); methysergide (MET).

Figure 7

ETO increased the c-fos expression in medullary respiratory areas. Photomicrographs illustrating the c-Fos immunoreactivity after DMSO (A-D) and ETO (E-L) exposure in the c/mNTS (A, E and I), the VLM (B, F and J), the obscurus (C, G and K) and pallidus (D, H and L) raphe nuclei. Scale bar = 100µm. Nucleus of the tractus solitarius, commissural and median parts (c/mNTS) and ventrolateral part (vlNTS); dorsal motor nucleus of vagus (DMX); hypoglossal nucleus (XII); ambiguus

nucleus (Amb); ventrolateral medullary reticular nucleus (VLM); obscurus (ROb) and pallidus (RPa) raphe nuclei; etonogestrel (ETO).

Figure 8

Catecholaminergic character of c-FOS-positive cells under ETO. (A and D) Drawings illustrating the distribution of cells immunoreactive for c-FOS alone and for both c-FOS and TH in the c/mNTS (A) and VLM (D) after ETO exposure (0.05µM); Scale bar = 100µm; white and black point represent respectively c-FOS-positive neurons and c-FOS-positive neurons also immunoreactive for TH. (B and E) Photomicrographs of sections double-immunolabelled for c-FOS and TH in c/mNTS (B) and VLM (E); Scale bar = 100µm; (C and F) Photomicrographs representing an enlargement of B and E; Scale bar = 10µm. Nucleus of the tractus solitarius, caudal and median parts (c/mNTS); ventrolateral medullary reticular nucleus (VLM); tyrosine hydroxylase (TH); ETO (etonogestrel).

Figure 9

Serotoninergic character of c-FOS-positive cells under ETO. (A and D) Drawings illustrating the distribution of cells immunoreactive for c-FOS alone and for both c-FOS and 5-HT in the pallidus and obscurus raphe nuclei; Scale bar = 100µm; white and black point represent respectively c-FOS-positive neurons and c-FOS-positive neurons also immunoreactive for 5-HT. Photomicrographs of sections double-immunolabelled for c-FOS and 5-HT in the pallidus (B and E) and obscurus (C and F) raphe nuclei after 0.05µM (B and C) or 2µM (E and F) ETO-normal pH-aCSF exposure; Scale bar = 10µm; etonogestrel (ETO); serotonin (5-HT).

Table 1

c-fos expression in medullary structures of *ex vivo* preparations.

Values are expressed as total number of c-FOS positive cells per structure ± SEM. * indicates a significant increase in total number of c-FOS positive cells per structure compared to DMSO values. # indicates a significant difference between 0.05 and 2µM of ETO. Kruskall-Wallis – Dunn post test. *$p < 0.05$, **$p < 0.01$, ***$p < 0.001$, $^{###}p < 0.001$. Nucleus of the tractus solitarius, commissural and median parts (c/mNTS), ventrolateral part (vlNTS); ventrolateral medullary reticular nucleus (VLM); pallidus raphe nucleus, caudal part (cRPa) and rostral part (rRPa); obscurus raphe nucleus, caudal part (cROb) and rostral part (rROb); magnus raphe nucleus (RMg); hypoglossal nucleus (XII); facial nucleus (7N); retrotrapezoid nucleus/parafacial respiratory group (RTN/pFRG); parapyramidal area (PP).

Table 1. *c-fos* expression in medullary structures of *ex vivo* preparations

	DMSO	ETO	
		0.05µM	2µM
	n = 8	*n = 12*	*n = 12*
c/mNTS	37.6 ± 11.7	120.7 ± 28.0*	28.1 ± 6.8$^{\#\#\#}$
vlNTS	6.7 ± 2.6	4.5 ± 0.8	3.8 ± 1.0
VLM	90.3 ± 21.1	253.5 ± 49.5*	225.3 ± 44.0*
cRPa	35.6 ± 8.3	56.5 ± 6.3	68.5 ± 9.1*
rRPa	14.0 ± 1.8	29.8 ± 4.9*	24.3 ± 2.8
cROb	43.9 ± 16.6	135.1 ± 14.9*	194.7 ± 36.6***
rROb	3.8 ± 1.7	48.5 ± 9.9***	35.5 ± 7.6**
RMg	9.4 ± 1.7	11.8 ± 2.8	9.2 ± 2.3
XII	19.3 ± 3.3	140.2 ± 35.7**	96.6 ± 19.8**
7N	134.0 ± 7.6	181.1 ± 10.8*	213.5 ± 18.5**
RTN/pFRG	6.3 ± 0.9	7.3 ± 1.4	8.5 ± 1.3
PP	8.8 ± 2.8	10.5 ± 1.7	13.5 ± 2.5

Values are expressed as total number of c-FOS positive cells per structure ± SEM. * indicates a significant increase in total number of c-FOS positive cells per structure compared to DMSO values. # indicates a significant difference between 0.05 and 2µM of ETO. Kruskall-Wallis – Dunn post test. *$p < 0.05$, **$p < 0.01$, ***$p < 0.001$, $^{\#\#\#}p < 0.001$. Nucleus of the tractus solitarius, commissural and median parts (c/mNTS), ventrolateral part (vlNTS); ventrolateral medullary reticular nucleus (VLM); pallidus raphe nucleus, caudal part (cRPa) and rostral part (rRPa); obscurus raphe nucleus, caudal part (cROb) and rostral part (rROb); magnus raphe nucleus (RMg); hypoglossal nucleus (XII); facial nucleus (7N); retrotrapezoid nucleus/parafacial respiratory group (RTN/pFRG); parapyramidal area (PP).

Figure 1 (1.5 column)

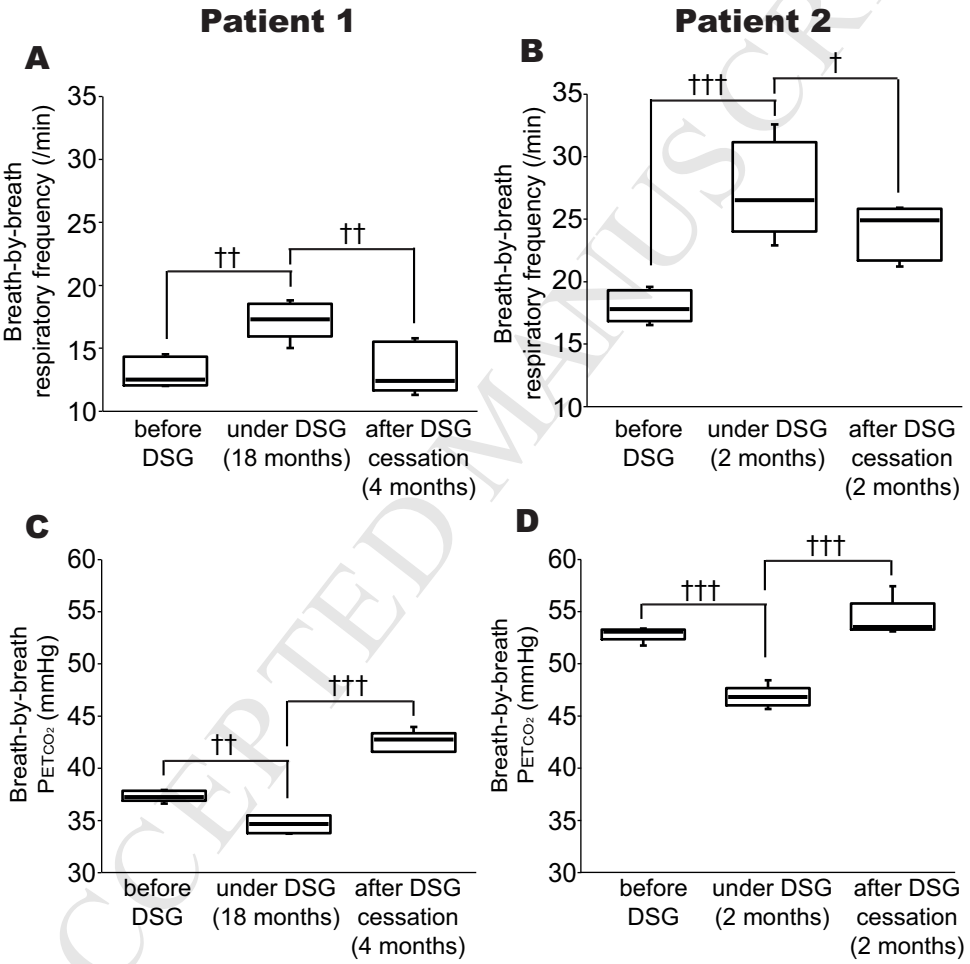

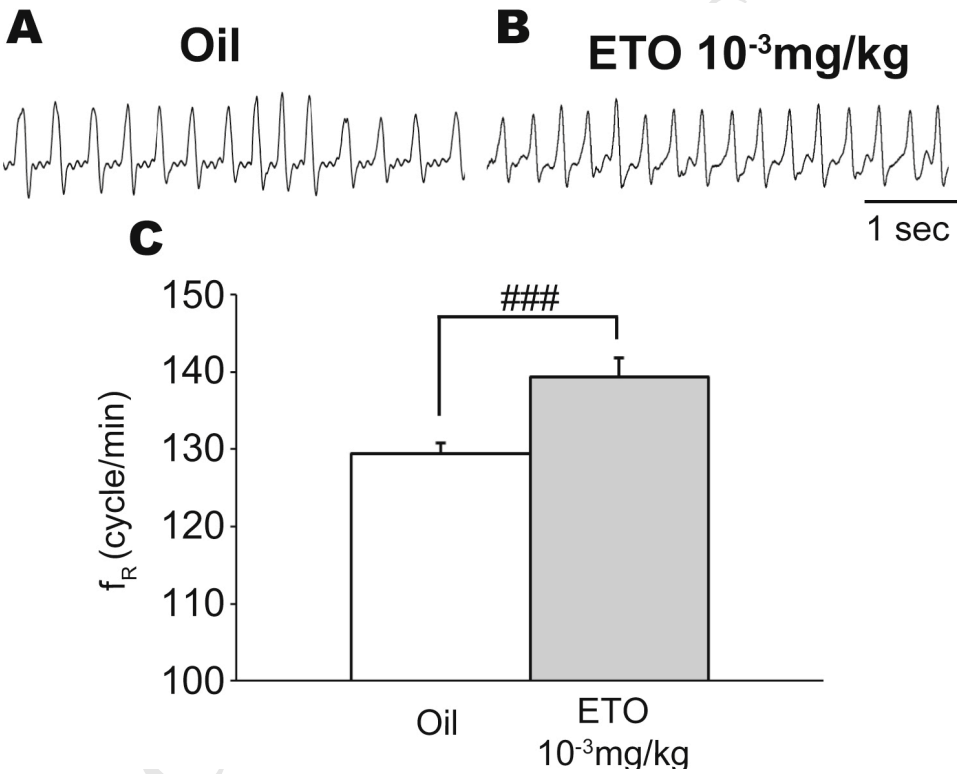
A
Oil
B
ETO 10-3mg/kg
1 sec
C
###
150
140
130
120
110
100
fR (cycle/min)
Oil
ETO
10-3mg/kg

Figure 3 (double column)

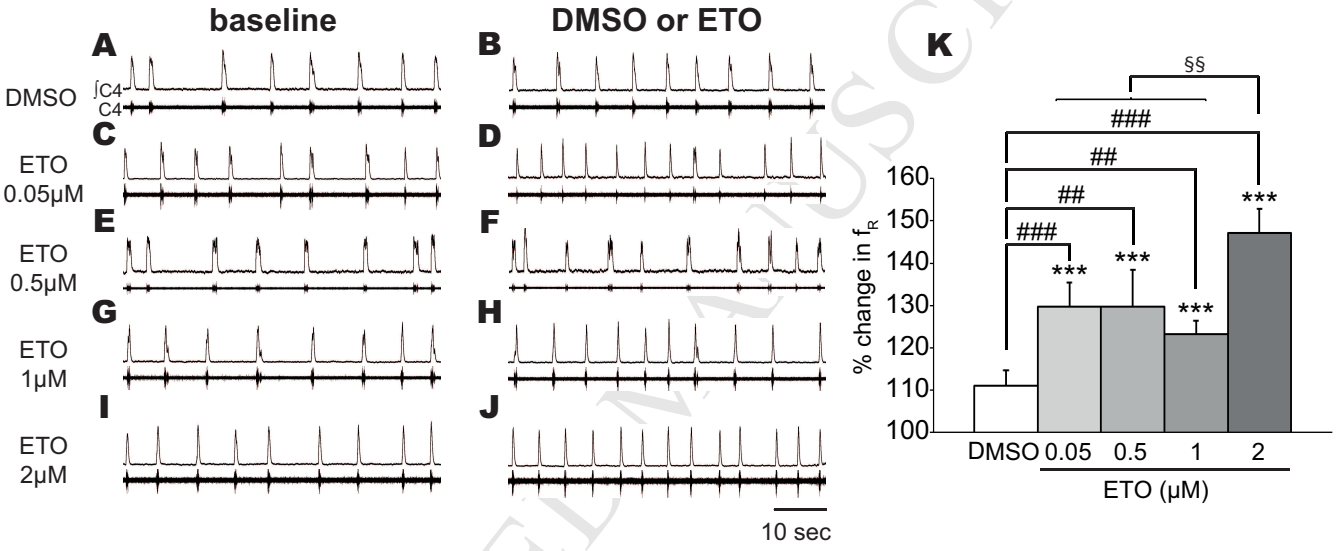

Figure 4 (double column)

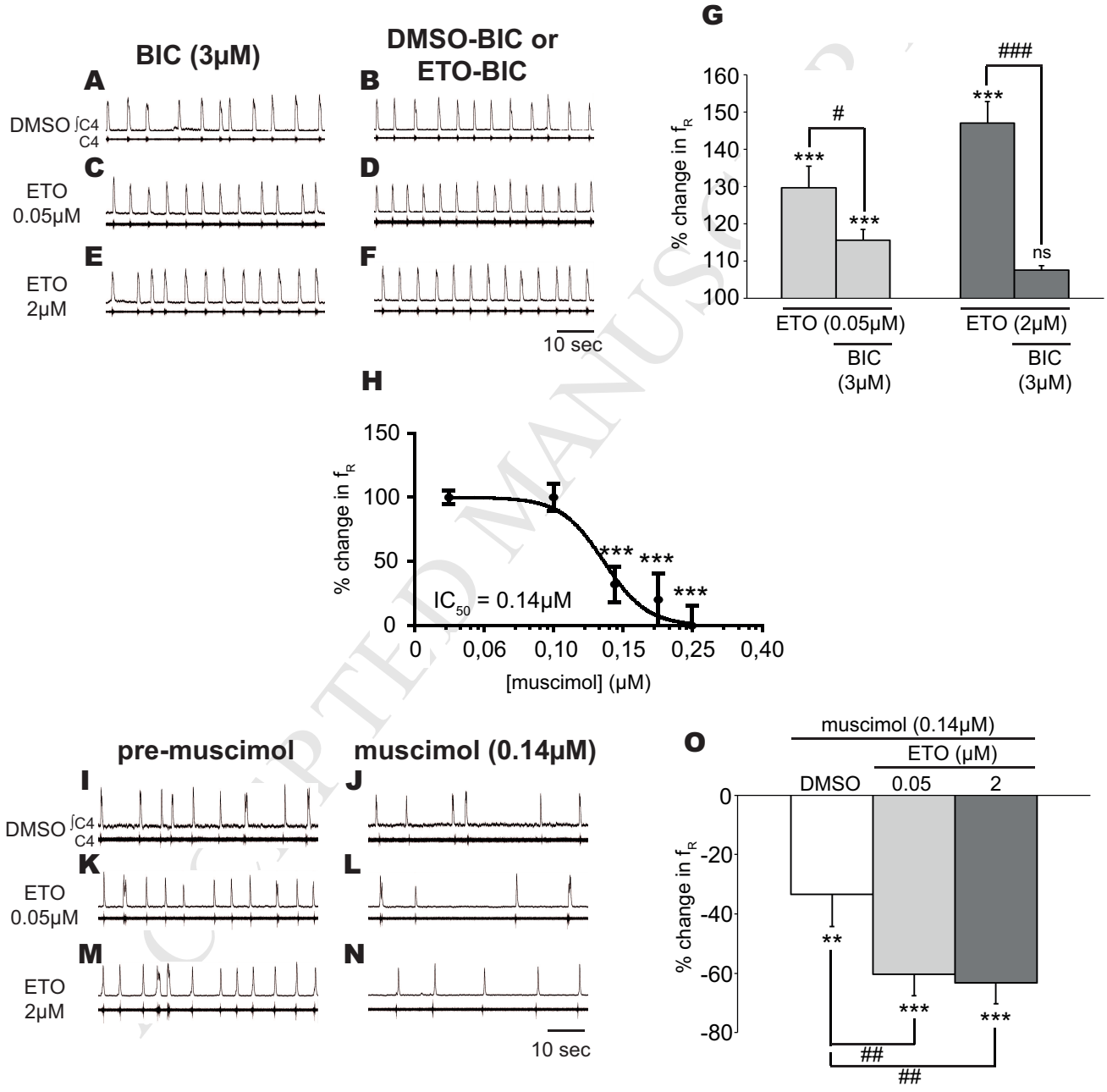

Figure 5 (double column)

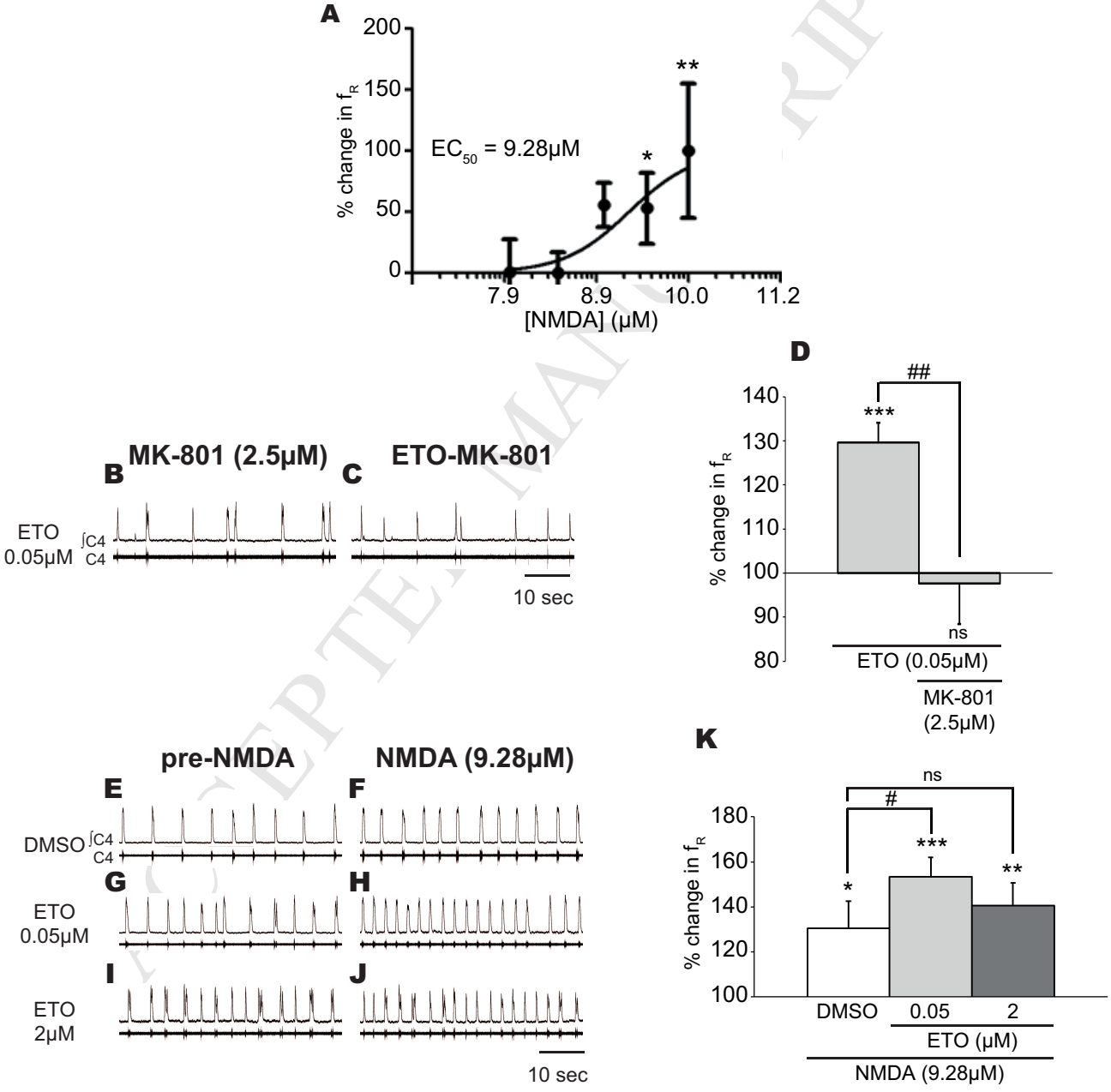

Figure 6 (single column)

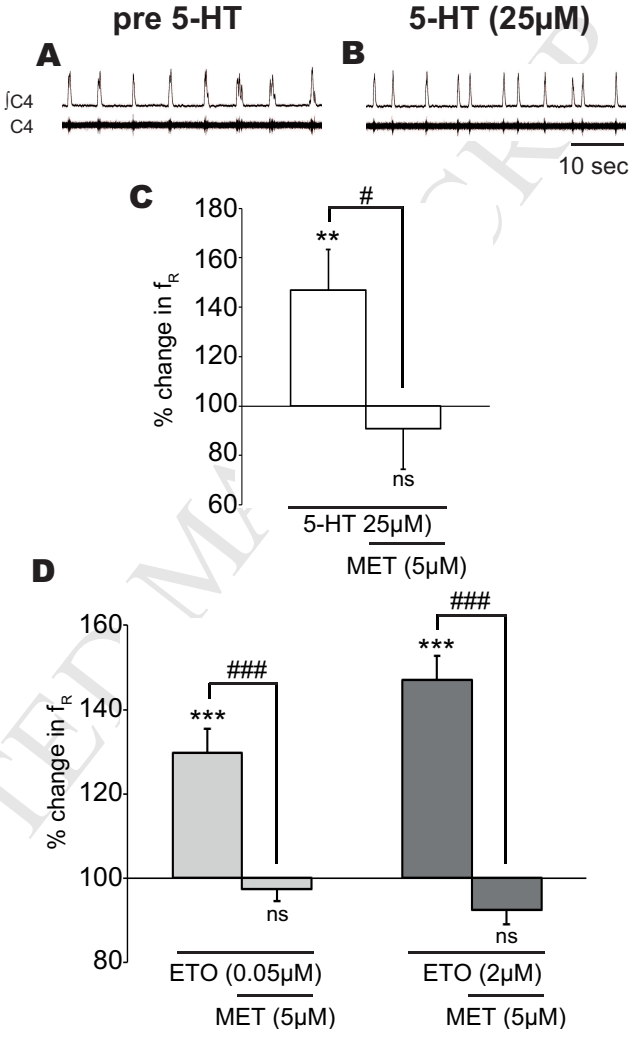

Figure 7 (double column)

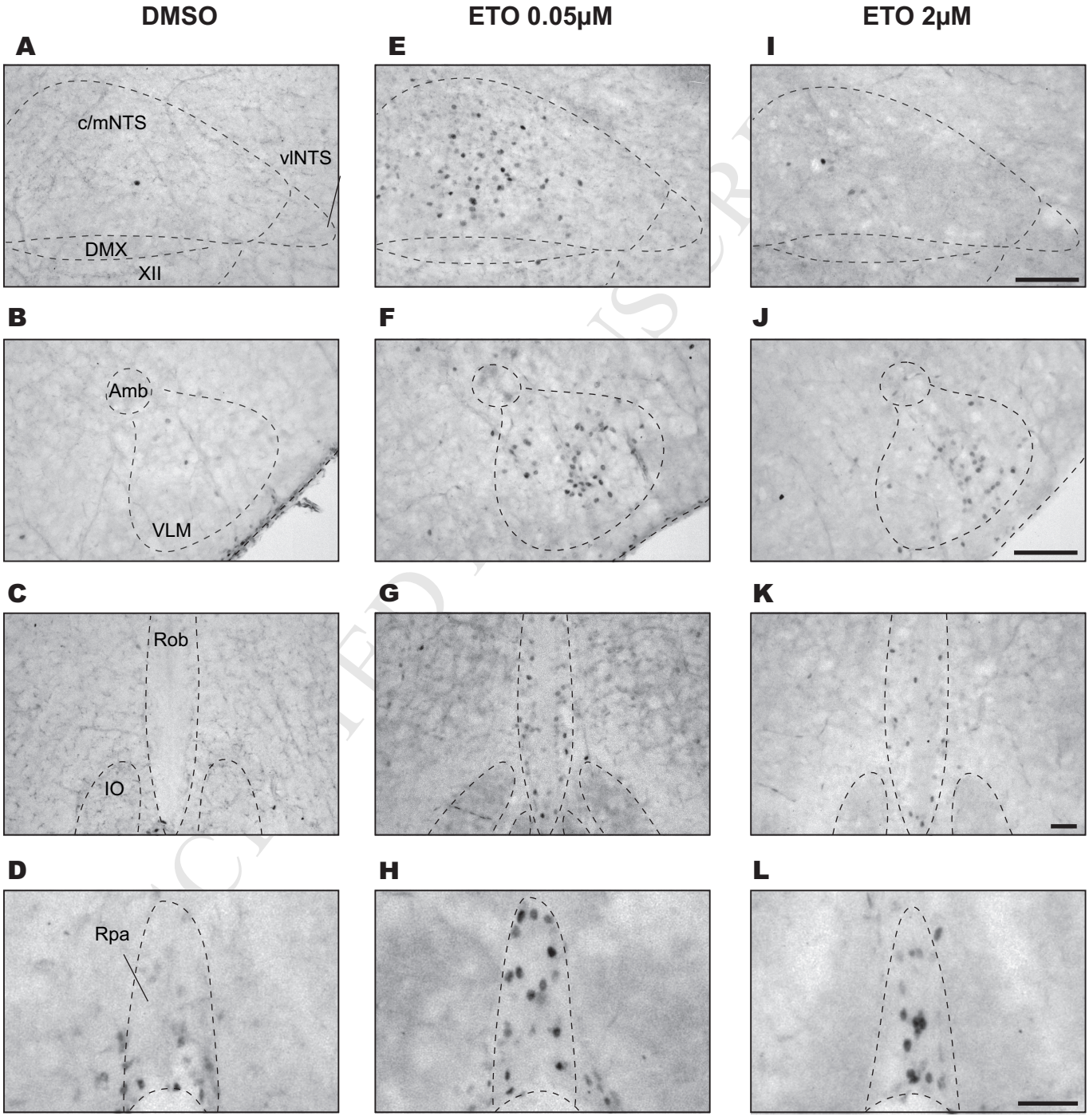

Figure 8 (single column)

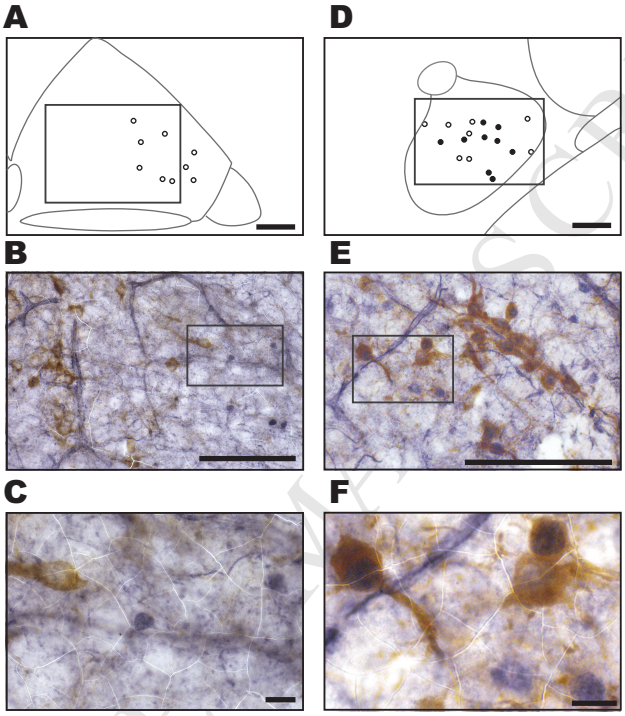

Figure 9 (1.5 column)

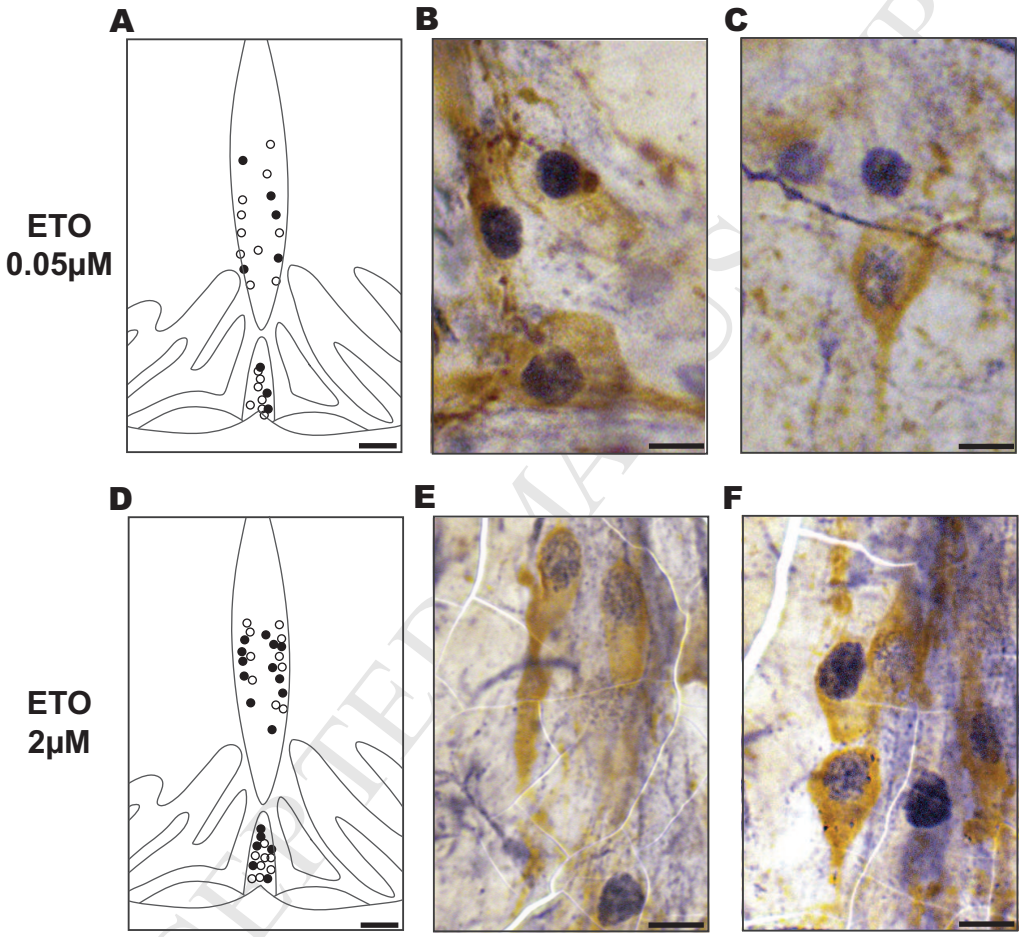

Highlights

-Desogestrel enhances basal ventilation in Ondine's curse

-Etonogestrel increased respiratory frequency by medullary mechanisms

-$GABA_A$ and NMDA receptors are involved in the respiratory effect of etonogestrel

-5-HT systems are implicated on the effect of etonogestrel on basal ventilation

-Combining 5-HT and desogestrel may constitute a therapeutic utility in Ondine's curse